

## Analysis of deformation paths in shear zones

By C. W. PASSCHIER, Utrecht\*)

With 9 figures

### Zusammenfassung

Die Geometrie duktiler Scherzonen kann dazu verwendet werden, regionale tektonische Probleme zu lösen, sofern der im Material abgebildete Deformationsweg dieser Zonen genügend verstanden wird. Der Flow in vielen Scherzonen mag sich aus einfacher Scherung ableiten lassen, daher genügen Daten über den letzten Deformationszustand wie z. B. der finite Strain und die Volumenänderung nicht für die Rekonstruktion des Deformationsweges, auch nicht bei konstanten Fließparametern während der fortschreitenden Deformation. Zusätzliche Daten über die Verwirbelungszahl (Rotationszahl) sind nötig. Sie lassen sich ableiten aus verschiedenartigen Gefügeelementen wie Gruppen gefalteter-boundinierter Gänge, rotierten Porphyroblasten und »verklebten«, starren Objekten. Vorgestellt werden anhand von Gefügedaten Konstruktionen am Mohr'schen Spannungskreis zur Bestimmung der Deformationsparameter, um damit den Deformationsweg graphisch darzustellen und daraus die Fließparameter abzuleiten. Änderungen in der Rotationszahl (Vorticity) oder der Geschwindigkeit in der Volumenänderung während progressiver Deformation erlauben den Deformationsweg zumindest teilweise zu rekonstruieren. Verwendung finden hierbei diejenigen Gefügeelemente, die sowohl die durchschnittliche Deformation als auch die letzten Deformationsereignisse registriert haben.

### Abstract

The geometry of ductile shear zones can be used to solve problems of regional tectonics if the deformation path of material in the zones is sufficiently understood. Flow in many shear zones may have deviated from simple shear and consequently data on the final deformation state such as finite strain and volume change are insufficient for reconstruction of the deformation path, even if flow parameters were constant during progressive deformation. Additional information on the flow vorticity number is also needed and can be obtained from fabric elements such as sets of folded-boudinaged veins, rotated porphyroblasts and blocked rigid objects. Mohr circle constructions are presented as a tool to calculate deformation parameters from fabric data, to represent the deformation path graphically and to reconstruct flow parameters from the shape

of this path. If the vorticity number or the volume change rate changed during progressive deformation, the deformation path can be partly reconstructed using sets of fabric elements which register mean and final values of these parameters.

### Résumé

La géométrie des shear zones ductiles peut être utilisée pour résoudre des problèmes de tectonique régionale, pour autant que l'histoire de la déformation des matériaux de ces zones soit suffisamment bien comprise. Il peut arriver, dans beaucoup de shear zones, que le processus ductile se soit écarté du modèle du glissement simple et qu'en conséquence, les caractères finals de la déformation, tels que l'ellipsoïde de la déformation finie, ou le changement de volume, s'avèrent insuffisants pour pouvoir reconstruire l'histoire de la déformation et ce, même si les paramètres de fluage sont restés constants au cours du processus. Il est alors nécessaire de disposer d'informations supplémentaires quant à la vorticit ; ces informations peuvent  tre fournies par certains  l ments structuraux tels que des groupes de veines pliss es-boudin es, des porphyroblastes qui ont tourn  et des objets rigides bloqu s. Au moyen de constructions appliqu es au cercle de Mohr, il est possible de calculer les param tres de la d formation   partir des donn es structurales, de repr senter graphiquement l'histoire de la d formation et de retrouver les param tres de fluage   partir de la forme de cette repr sentation. Si, au cours de la d formation progressive, la vorticit  ou le taux de variation de volume se modifient, l'histoire de la d formation peut  tre reconstitu e partiellement par l'utilisation de groupes d' l ments structuraux qui enregistrent les valeurs moyenne et finale de ces param tres.

### Краткое содержание

Если при исследовании пород линия деформации пластичных зон скола достаточно хорошо изучена, то на основании формы этих зон скола удается решить тектонические проблемы регионального характера. Направление течения во многих зонах скола можно вывести на основании простого смещения и, следовательно, по состоянию их последней деформации. Однако, конечная деформация и измене-

\*) Author's address: C. W. PASSCHIER, Instituut voor Aardwetenschappen, Budapestlaan 4, Utrecht, The Netherlands.

ние объема оказываются недостаточными для реконструкции пути деформации, если даже параметры потока остаются неизменными во время последовательно усиливающейся деформации. Необходимы еще дополнительные данные о скорости течения, которую можно вывести из элементов текстуры, как напр.: систем жил, смятых в складку и преобразованные в будины закрученных порфириобластов и «заклиненных» неподвижных объектов. Из данных строения текстуры в поле напряжения Мора определяют параметры деформации, по которым строят графики пути ее течения. Колебания числа вращения, или скорости изменения объема во время продолжающейся деформации разрешают, хотя бы частично, реконструировать пути ее протекания. При этом опираются на те структурные элементы, которые отмечены, как при деформации всей данной породы в среднем, так и во время последнего процесса деформации.

### Introduction

Ductile shear zones, which are common structural elements at mid to deep crustal levels, are the effect of strong flow partitioning in rocks. They can be used for the reconstruction of large-scale tectonics in orogenic belts since they accommodate a large part of the regionally imposed deformation and are relatively easy to map or to detect on seismics (e.g. CAZES et al., 1985; SMITHSON et al., 1979; SMYTHE et al., 1982; PASSCHIER, 1986a). Flow in shear zones is often assumed to approach simple shear parallel to zone boundaries because of monoclinic shape fabric elements and high finite strain in the zone, which is absent or less pronounced in the wall rock. In fact, only shear zones with perfectly undeformed wall rocks and absence of volume change can satisfy this assumption. In most natural shear zones flow was not necessarily a simple shear and flow parameters may have changed during the deformation. This is a serious problem, since superficially similar fabric patterns in a shear zone and its wall rock may have formed by a large variety of different flow patterns in completely different large scale tectonic settings (Fig. 1); a detailed analysis of the deformation path in the shear zone and if possible in the wall rock is needed to distinguish between them. This paper gives an outline of the way in which fabric data from shear zones can be used to reconstruct at least some aspects of the deformation path, and explains the influence of flow parameters on the shape of the path.

### Flow patterns

Homogenous flow in a volume of rock can be described in a purely geometrical way, regardless of the

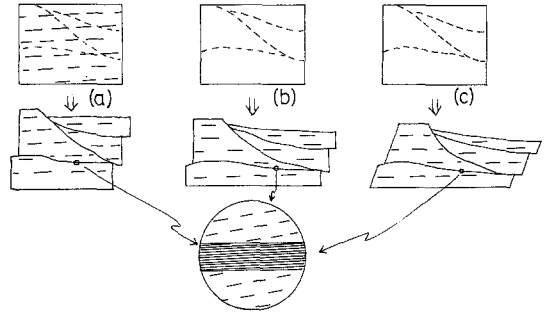


Fig. 1. Three different macroscopic deformations with formation of shear zones lead to identical shear zone/wall rock foliation geometry. In (a), an older foliation is cut by shear zones with a rigid wall rock. In (b) and (c) the original material is undeformed. Analysis of the deformation path in the shear zones can help to distinguish these situations.

presence of anisotropies or the rheology of the material involved, by equations of the type:

$$\dot{X}_i = L_{ij} \cdot X_j$$

where  $L$  is the velocity gradient tensor,  $X$  a position in space and  $\dot{X}$  the rate of displacement of a particle at that position (MALVERN, 1969; LISTER & WILLIAMS, 1983; PASSCHIER, 1986b). The description can be restricted to plane strain or two dimensional flows if the vorticity vector of the flow remains parallel to the intermediate instantaneous stretching axis, and if stretching rates along this axis are negligible. This is a reasonable assumption for many shear zones since (1) the intersection lineation of various foliations usually parallels the symmetry axis of microstructures with monoclinic shape symmetry such as shear band cleavage, mica fish or feldspar porphyroclast systems (SIMPSON & SCHMID, 1983; PASSCHIER, 1986a; PASSCHIER & SIMPSON, 1986) and (2) stretch parallel to this symmetry axis is usually of minor importance. A simplistic, two dimensional approach assuming absence of stretching in the direction of the vorticity vector is adopted throughout this paper to restrict the complexity of the model while illustrating the techniques that can be used; more realistic, complex three dimensional flows can be approached along the same lines if sufficient data are available.

Flow in a plane normal to the vorticity vector can be represented by  $L$  in a  $2 \times 2$  matrix with instantaneous stretching axes (ISA) fixed at  $45^\circ$  to an external reference frame, as (PASSCHIER, 1987a):

$$L = \begin{bmatrix} a & s + W_n \cdot s \\ s - W_n \cdot s & a \end{bmatrix}$$

Any other orientation of ISA is equally valid provided they are fixed in the external reference frame, but leads to more complex tensor components (PASSCHIER, 1987a). Alternatively,  $L$  can be represented as a Mohr circle (Fig. 2; LISTER & WILLIAMS, 1983). Cartesian coordinates of each point on the circle represent the angular velocity  $\omega$  and the stretching rate  $\dot{\epsilon}$  of a material line (LISTER & WILLIAMS, 1983; PASSCHIER, 1986b).  $s_1$  and  $s_2$  represent instantaneous stretching rates along ISA,  $s$  is the mean instantaneous stretching rate  $s = (s_1 - s_2)/2$  and  $a$  the volume change rate  $a = s_1 + s_2$ , provided stretch in the direction of the vorticity vector is negligible. For isochoric flow  $a = 0$ . In Mohr circle presentation,  $s$  is the circle radius,  $a$  the deviation of the Mohr circle center from the vertical axis and  $W/2$  the deviation from the horizontal axis (Fig. 2), where  $W$  is the flow vorticity (MALVERN, 1969; TRUESDELL, 1954).  $W_n$  is the neutral vorticity number  $W_n = W/2s$ .  $W_n$  does not generally coincide with the kinematic vorticity number of TRUESDELL  $W_k$  (TRUESDELL, 1954; MEANS et al., 1980) except if  $a = 0$ . Intersection points of the Mohr circle with the horizontal  $\omega = 0$  axis represent material lines in the flow which are instantaneously irrotational with respect to ISA, also called »flow apophyses« (PASSCHIER, 1986b; RAMBERG, 1975a, 1975b). Material points on the apophyses move in straight lines towards or away from the origin of the reference frame. Flow apophyses have a fixed symmetrically arranged position with respect to ISA and are useful in graphs illustrating flow patterns (Fig. 2a). The angle between flow apophyses is a function of  $W_n$  only and is independent of  $a$  (Fig. 2; PASSCHIER, 1986b; BOBYARCHICK, 1986; RAMBERG, 1975a, 1975b).

In contrast to the description of flow, incremental or finite deformation is expressed in equations of the type:

$$X'_p = F_{pq} \cdot X_q$$

$F$  being the position gradient tensor,  $X$  the original position of a particle, and  $X'$  its final position (MALVERN, 1969; MEANS, 1982). The incremental position gradient tensor  $F_i$  is derived from  $L$  by integration as:

$$F_i = \int L \cdot dt = \begin{bmatrix} a \cdot \Delta t & (s + W_n \cdot s) \Delta t \\ (s - W_n \cdot s) \Delta t & a \cdot \Delta t \end{bmatrix}$$

For flow with invariable parameters  $s$ ,  $a$  and  $W_n$ , the finite position gradient tensor  $F$  can be derived from  $F_i$  by the eigenvector method (KREIDER, 1972) or by sequential multiplication of  $n$  tensors  $F_i$  (ELLIOTT, 1972), rewriting the resulting binomial series as:

$$F^n = \lim_{\Delta t \rightarrow 0} \frac{\Delta t}{(n \cdot \Delta t = t)} (F_i)^n = \exp(L \cdot t)$$

If  $0 \leq W_n < 1$  this can be written as (MCKENZIE, 1979; PASSCHIER, in prep):

$$F_i^{(0 \leq W_n < 1)} = \exp(a \cdot t) \begin{bmatrix} \cosh(s \cdot t \cdot \sqrt{1 - W_n^2}) \cdot \sqrt{\frac{1 + W_n}{1 - W_n}} \cdot \sinh(s \cdot t \cdot \sqrt{1 - W_n^2}) \\ \sqrt{\frac{1 - W_n}{1 + W_n}} \cdot \sinh(s \cdot t \cdot \sqrt{1 - W_n^2}) \cdot \cosh(s \cdot t \cdot \sqrt{1 - W_n^2}) \end{bmatrix}$$

If  $W_n = 1$  (simple shear)  $F_i$  can be written as:

$$F_i^{(W_n = 1)} = \exp(a \cdot t) \begin{bmatrix} 1 & 2s \cdot t \\ 0 & 1 \end{bmatrix}$$

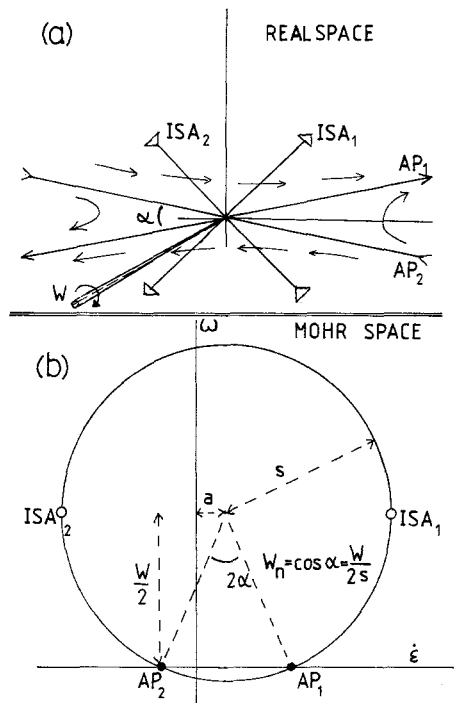


Fig. 2. Representation of a general flow field in real space (a) and Mohr space (b); ISA — instantaneous stretching axes; AP — flow apophysis;  $W$  — vorticity;  $s$  — mean instantaneous stretching rate;  $a$  — instantaneous volume change;  $\alpha$  — angle between flow apophyses. Cartesian coordinates of each point on the Mohr circle represent angular velocity ( $\omega$ ) and instantaneous stretching rate ( $\dot{\epsilon}$ ) of a material line in real space.

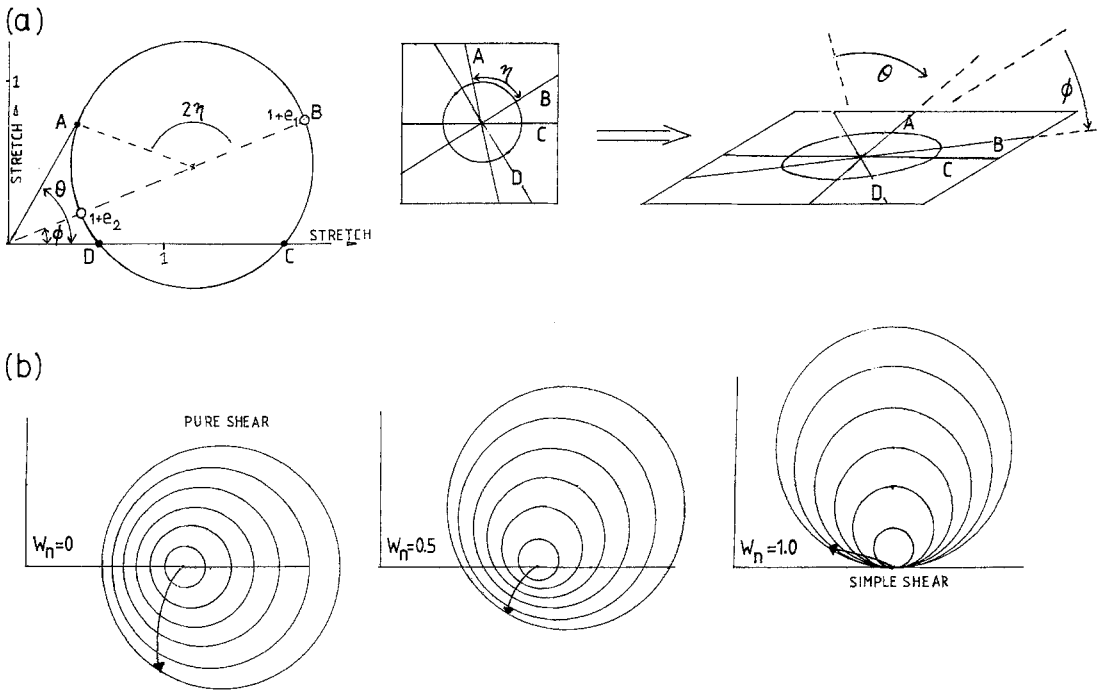


Fig. 3. (a) Mohr circle for the finite position gradient tensor  $F_t$ . Polar coordinates of each point on the circle represent stretch and rotation of a material line in real space as shown on the right; (b) progressive deformation for three different vorticity numbers  $W_n$ , illustrated in Mohr space by series of  $F_t$ -circles with increasing diameter. For each case, flow is homogeneous with constant  $a$  and  $W_n$ . Solid arrows show the different stretch/rotation histories in each case for a material line which was originally oriented at  $30^\circ$  to the instantaneous shortening axis.

Both matrices for  $F_t$  given above can be represented in a Mohr space as off-axis circles of a type different to that used to illustrate  $L$  (Fig. 3; BOBYARCHICK, 1986; MEANS, 1983; DE PAOR, 1983; DE PAOR & MEANS, 1984). For this type of Mohr construction, stretch is plotted on both axes and *polar coordinates* of a point on the  $F_t$ -circle represent the stretch and rotation of a material line in real space (Fig. 3a; MEANS, 1982, 1983). Progressive deformation can be illustrated in Mohr space by circles of increasing diameter which shift from a stretch value 1 on the horizontal axis into the space (Fig. 3b; BOBYARCHICK, 1986; PASSCHIER, in press). The shape of the path along which the Mohr circle center moves is a function of  $s$ ,  $a$ ,  $W_n$  and their change with time. For invariable coefficients of  $L$ , such paths are regular curves as shown in Figure 4 for isochoric flow.

The radius of the Mohr circle ( $R$ ) is a simple function of the volume change factors ( $a, t$ ) or  $\Delta V$  and a factor  $T$  representing the distance of the Mohr circle to the origin (Fig. 5). For any point on one of the »Mohr-circle center paths« of Figure 4,  $R$  can be

calculated and the Mohr circle constructed if sufficient data on volume change up to that point are available. Since the Mohr circle represents the full position gradient tensor, the stretch rotation of any material lines at that stage can now be determined. This means that the path of the Mohr circle center in Mohr space (Fig. 4) is a useful presentation of the »deformation path« (ELLIOTT, 1972); it contains the full information necessary to find the current position gradient tensor  $F_t$  at any stage of the deformation, provided volume change is known for that stage. The shape of the path for naturally deformed rocks will usually deviate from the standard curves in Figure 4; the shape of the path can reflect changes in flow parameters  $s$ ,  $a$  and  $W_n$  during progressive deformation, e.g. a change from pure shear to simple shear flow. With the deformation path known, it is possible to follow the stretch and rotation history of any individual material line, e.g. a shear zone boundary during the deformation (Fig. 3b), and thereby predict possible flow regimes in the wall rock. This makes an analysis of the deformation path useful for many shear zones.

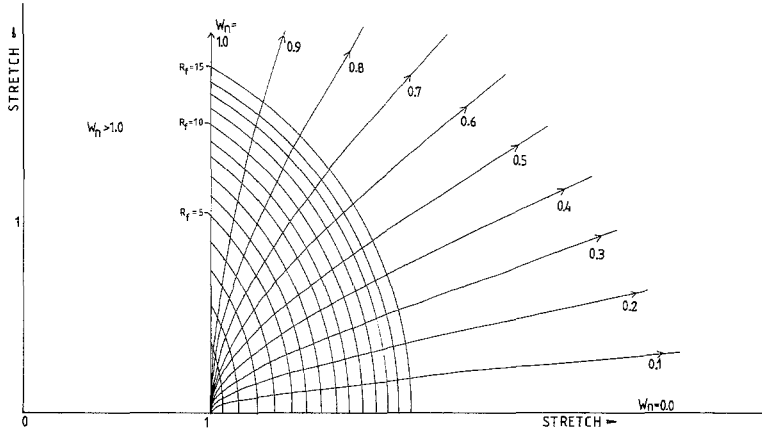


Fig. 4. Paths traced by the center of the  $F_I$ -Mohr circle during progressive deformation by isochoric flow with invariable  $W_n$ . Concentric curves are Mohr circle center positions for specific  $R_f$ -values.

**Analysis of the deformation path**

For a complete analysis of the deformation path in a volume of rock, the path of the Mohr circle center for  $F_I$  must be fully reconstructed. If flow parameters  $s$ ,  $a$  and  $W_n$  did not change during the deformation, it is sufficient to determine  $F_I$  for the final state of the deformation, since this automatically decides which of the curves as in Figure 4 has been followed.  $F_I$  can be reconstructed by finding the size and position of its Mohr circle, e.g. by calculation of  $T$ ,  $R$  and  $Q$  from fabric data (Fig. 5b) or by determination of stretch and rotation of at least three random material lines, which will lie on the circle (PASSCHIER & URAL, in prep).  $R_f$ , the axial ratio of the finite strain ellips and  $\Delta V$ , the volume change, are always sufficient to determine  $T$  and  $R$  for any type of deformation path (Fig. 5b). If flow was known to be a pure shear, these data are sufficient to construct the Mohr circle since  $Q = 0$ . For persistent simple shear flow, knowledge of  $R_f$ ,  $\Delta V$  and sense of shear are sufficient since  $Q = R$ . For more general flow types (Fig. 5b),  $Q$  must be calculated from  $R_f$ ,  $\Delta V$  and  $W_n$ . Methods to determine  $W_n$  and  $Q$  are outlined below. With the Mohr circle reconstructed, matrix components of  $F_I$  can be read off following the method described by MEANS (1982, 1983).

**Markers for  $W_n$**

The rotation of material lines during deformation with respect to a randomly chosen external reference frame consists of a vortical rotation component with respect to ISA, and a spin component of ISA in the external reference frame (LISTER & WILLIAMS, 1983).

Many fabric elements only store information on the vertical rotation component, and can therefore be used to calculate  $W_n$  of flow during the deformation. It

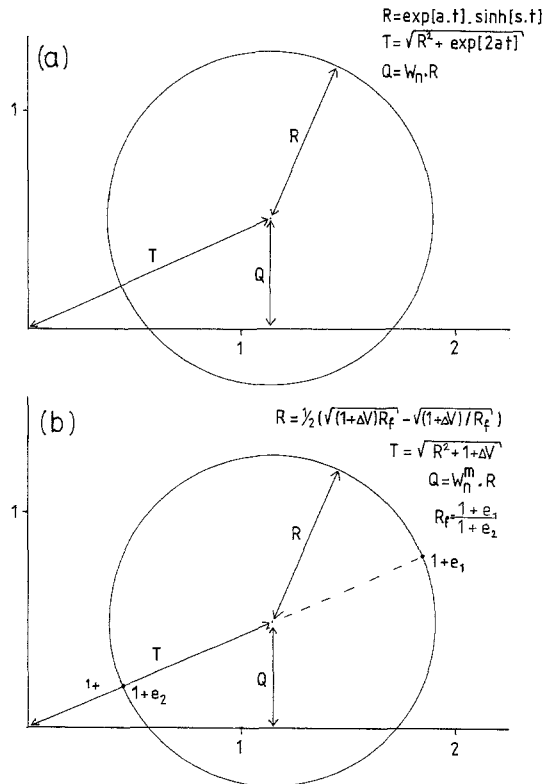


Fig. 5. Representation of parameters  $T$ ,  $R$  and  $Q$  of an  $F_I$ -Mohr circle in terms of: (a) flow parameters  $a$ ,  $s$ ,  $W_n$  and time  $t$ ; (b) finite deformation parameters  $R_f$ ,  $\Delta V$  and »means« vorticity number  $W_n$ .

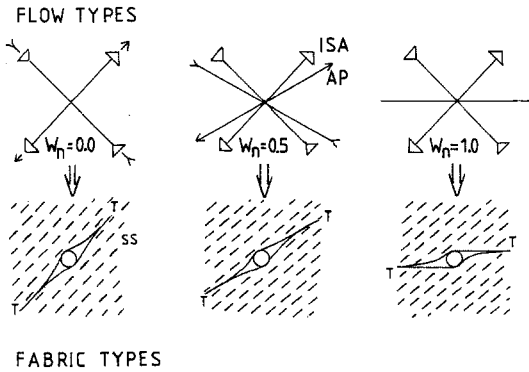


Fig. 6. Schematic illustration of the orientation dependence of certain fabric elements on specific directions in the flow; elements such as tails of recrystallized material (T) around porphyroclasts rotate towards parallelism with the extensional apophysis (AP) while steady state fabrics (SS) are fixed with respect to instantaneous stretching axes (ISA). This contrast leads to a dependence of fabric geometry on flow vorticity number.

has long been known (Fig. 6) that some fabric elements develop in a fixed orientation with respect to ISA, such as quartz preferred orientation fabrics (LISTER & HOBBS, 1980), steady state foliations (MEANS, 1981), symmetry axes of rigid objects blocked in the flow (GHOSH & RAMBERG, 1976; FREEMAN, 1985; PASSCHIER, 1987b) and fibres in crack-seal veins (DURNEY & RAMSAY, 1973). Other fabric elements, however, are linked to the orientation of the finite strain ellipsoid, which rotates with progressive deformation from the position of the extensional ISA to the extensional flow apophysis and trends to parallelism with this apophysis at high finite strains (Fig. 6). Such fabric elements of the second type include shape fabrics (planar and linear), pressure solution foliations and passively rotating and stretching objects, lines and planes in the rock. Since the angle between ISA and apophyses is a function of  $W_n$  only, the difference in orientation between a set of fabric elements from the first and second group, combined with data on finite strain can be used to calculate  $W_n$  during the flow. Some examples of  $W_n$ -markers are (Fig. 7):

(1) The »finite strain method«, measuring the angle over which material lines coinciding with the finite strain axes have rotated with respect to ISA (Fig. 7a). In Mohr space this is the angle  $\beta$  between the circle center and the horizontal axis which can be plotted directly.  $W_n$  can be calculated following  $W_n = (T \cdot \sin \beta) / R$ .

(2) The »Ghosh method«, calculating  $W_n$  from the ratio of the total finite rotation of a spherical object with respect to ISA and the finite strain (Fig. 7b; GHOSH, 1987). The ratio only depends on  $W_n$ ,  $R_f$  and  $\Delta V$ .

This method can be applied to rocks with porphyroblasts which overgrew an older foliation (SCHONEVELD, 1977), though great care should be taken that only the rotation component with respect to ISA is measured, and not the relative rotation between rigid object and foliation, both rotating with respect to ISA. BELL (1985) outlined some of these problems.

(3) The »Talbot method« (TALBOT, 1970; HUTTON, 1982), using the distribution of shortened, extended, shortened/extended and extended/shortened lines in space at a specific finite strain magnitude (Fig. 7c). This distribution depends on  $W_n$ ,  $R_f$  and  $\Delta V$ . It is a powerful method which can be used in rocks containing sets of veins with a sufficient range of orientations and sufficient competency contrast with the matrix.

(4) The »blocked objects method« (GHOSH & RAMBERG, 1976; FREEMAN, 1985; PASSCHIER, 1987b), based on the fact that elongated objects can become stationary in flow types with  $0 \leq W_n < 1$  (Fig. 7d). The orientation of a blocked object with respect to ISA of the flow only depends on its axial ratio and  $W_n$  (Fig. 6). Populations of rigid objects in a ductilely deforming matrix in which a high finite strain has accumulated can be divided into a permanently rotating group with low aspect ratios and a blocked group with high aspect ratio (Fig. 7d). If both groups can be distinguished, e.g. by the shape of pressure shadows or recrystallized tails around them,  $W_n$  can be determined from (a) the axial ratio of objects at the »cut-off-point« between both groups and (b) the orientation of blocked objects of specific axial ratio with respect to a fabric element of the first or second type such as a compositional layering or a steady state foliation (PASSCHIER, 1987b). Method (a) seems most reliable at present (PASSCHIER, 1987b). The method only works if the matrix away from the rigid object deformed in a relatively homogeneous way. Significant flow partitioning around an object as envisaged by BELL (1985) would inhibit the use of the blocked object method.

(5) The »stair stepping method«, which can be applied for rigid porphyroclasts which recrystallize along the outer margin and develop tails of recrystallized material (SIMPSON & SCHMID, 1983; PASSCHIER & SIMPSON, 1986; Fig. 7e). Such tails stretch out from porphyroclasts at two different levels, parallel to the long axis of the finite strain ellipsoid to produce a »stair-stepping« geometry (Fig. 7e; LISTER & SNOKE, 1984; PASSCHIER & SIMPSON, 1986). The ratio of the distance between tails against the diameter of the central porphyroclast is expected to be a function of  $W_n$ .

(6) The »crystallographic fabric method«, using the fact that the distribution of crystal symmetry axes of a material deformed by crystalplastic deformation is a function, not only of deformation mechanisms and ac-

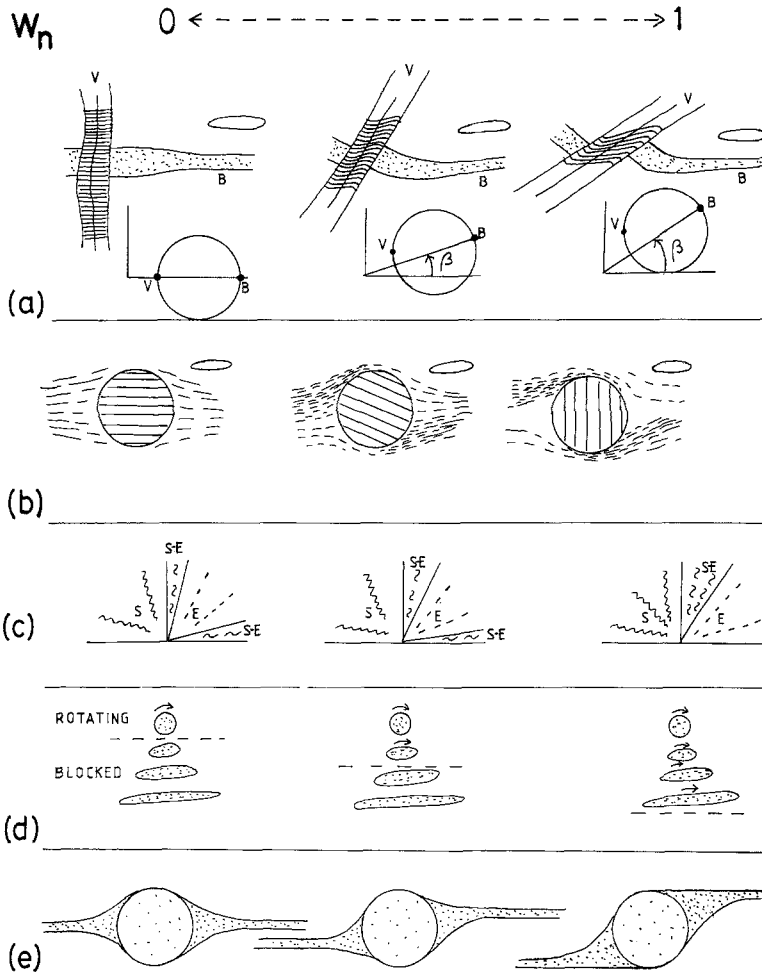


Fig. 7. Selection of fabric elements which can be used to calculate the vorticity number of the flow; (a) the angle of rotation  $\beta$  of a material line ( $B$ ) which coincides with the finite extension axis relative to ISA, determined from its rotation with respect to a fibrous vein system ( $V$ ); (b) rotation of a spherical rigid object with respect to ISA for a specific finite strain value; (c) distribution of shortened ( $S$ ), extended ( $E$ ) and first shortened/then extended ( $S-E$ ) veins in a deformed material; (d) range of axial ratios of rigid objects which are permanently rotating or which are irrotational (blocked) in the flow; (e) degree of stair stepping of tails of recrystallized material around rigid objects.

tive slip systems, but also of  $W_n$  (LISTER & HOBBS, 1980; DIETRICH & SONG, 1984, LAW et al., 1984; PLATT & BEHRMANN, 1986). This method may be difficult to calibrate, however.

(7) Methods involving crack-seal veins and foliation elements. If crack-seal veins can be shown to have grown parallel to the instantaneous extension axis during progressive deformation (DURNEY & RAMSAY, 1973), their orientation with respect to other fabric elements which trend towards parallelism with the extensional apophysis, e.g. compositional layering, will give a measure of  $W_n$ .

(8) Methods involving other fabric elements of the first and second type. The angle between fabric elements linked to instantaneous stretching axes, e.g.  $e$ -twins in calcite or steady state foliations, and others which trend towards the extensional apophysis, e.g. compositional layering is a function of finite strain and  $W_n$ . If sufficient data are available, this method could be calibrated to yield  $W_n$ .

#### Variable $W_n$

In cases where  $W_n$  varies with time, deformation paths as indicated by the movement of the Mohr cir-

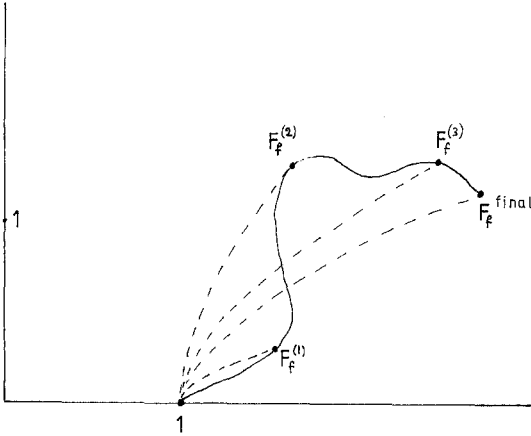


Fig. 8. Hypothetical deformation path for a volume of rock in which flow parameters changed with time, represented by the path which is traced by the center of the  $F_F$ -Mohr circle during progressive deformation. Each point on the path could also have been reached along one of the standard curves in Fig. 4 for invariable flow parameters. The  $W_n$ -value of the standard curve which leads to the final point on the path is the mean vorticity number  $W_n$  for the total deformation.

cle center in Mohr space can be rather complex (Fig. 8) and knowledge of the final  $F_F$  is no longer sufficient to predict the shape of the path. In the case of shear zones, a change in  $W_n$  during flow history has direct consequences on the deformation history of the wall rock, although in a single-phase shear zone with a homogeneous fabric distribution, changes were probably gradual and constrained by coupling between the

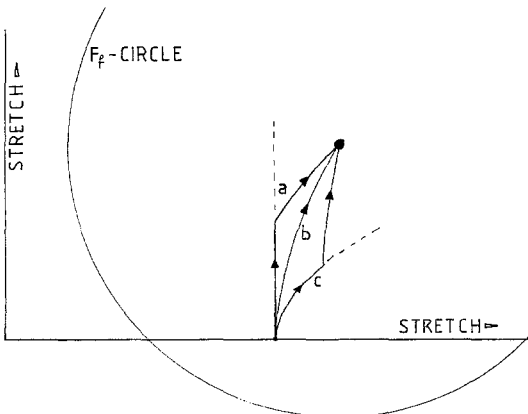


Fig. 9. Three paths of  $F_F$ -Mohr circle centers, representing different deformation paths all lead to the same final deformation state. Explanation in text.

deforming zone and the wall rock. The complex deformation path must therefore be optimally reconstructed if deformation in the wall rock is to be fully understood. Figure 8 shows how any position gradient tensor  $F_F$  on a complex deformation path at a specific stage of the deformation could also have been reached along a path with constant  $W_n$ . This  $W_n$  value differs for every  $F_F$  stage and constitutes the »mean« value of  $W_n$  up to that stage of deformation. A full reconstruction of the deformation path would require determination of  $R_i$ ,  $\Delta V$  and the »mean«  $W_n$  at successive stages of the deformation. In most geological situations this proves impossible. At best, partial reconstruction of a complex deformation path can be carried out in two steps: (1) determination of the »mean«  $W_n$  for the total deformation and construction of the final  $F_F$ -Mohr circle; (2) determination of first order deviations of the true deformation path from the »mean« path which leads to the final  $F_F$  position (Fig. 8). For the first step  $Q$  is calculated from the »mean« value of  $W_n$  during the deformation. Only the finite strain and the Ghosh methods can be directly applied to find this »mean« value, because they simply add rotation increments during the deformation. The other methods probably reequilibrate during the deformation and approach the last values of  $W_n$  reached.

First order deviations from a »standard« deformation path as in Figure 4 can probably be established in many deformed materials once the »mean«  $W_n$  has been established and  $F_F$  calculated for total deformation. Fabric elements formed during part of the deformation history, such as crack-seal veins or inclusion patterns in porphyroblasts can be used to determine »intermediate« points of the deformation path (Fig. 8) or results from different  $W_n$  markers, those for mean and reequilibrated values, can be compared. In Figure 9, three deformation paths have been plotted in Mohr space: (a) flow with  $W_n = 1.0$  during the first half and 0.4 during the second half of the deformation history (Fig. 9a); (b) flow with invariable  $W_n = 0.7$  (Fig. 9b); (c) flow with  $W_n = 0.4$  during the first half of the flow history and  $W_n = 1.0$  during the second half (Fig. 9c). For the values of  $s$  and  $t$  used in the calculation (0.1 and 10 for the entire deformation history), all three paths result in an identical finite position gradient tensor, i.e. at the same point in Mohr space. This means that the finite rotation and stretches of material lines along the three paths are equal, but that the rotation and stretch histories of these lines are different. The three paths could be distinguished by the use of different markers of  $W_n$ . The finite strain and Ghosh methods will give similar results ( $W_n = 0.7$ ) for all three paths, while the blocked object method would ideally give values of  $W_n = 0.7, 1.0$  and 0.4 as a result

of reequilibration to the last part of the deformation path. Combination of the finite strain or Ghosh methods and the blocked object method will show that for (a)  $W_n$  was decreasing during the deformation, for (b)  $W_n$  remained constant and for (c)  $W_n$  was increasing. This means that it should be possible in practice to determine whether the deformation path in Mohr space roughly coincided with a constant  $W_n$  history (b), or was situated in the domains above (a) or below (c) the constant  $W_n$  curve.

### Variable $s$ and $a$

Besides variations in  $W_n$ , a variable mean stretching rate  $s$  and volume change rate  $a$  may be common in nature. The effects of their variability on the finite fabric are much less noticeable, however. For progressive deformation with invariable  $W_n$ , changes in  $s$  result in periods of relatively fast or slow accumulation of deformation, i.e. in a change in velocity of the Mohr circle center in Mohr space without any deviations from the path for that particular  $W_n$  value as shown in Figure 4. Deformation paths as outlined above are not sensitive to absolute values of the mean stretching rate, or to changes therein during the deformation.

Changes in volume change rate  $a$  along a deformation path with constant or variable  $W_n$  steepens or flattens the path of the Mohr circle center, but does not affect the ratio  $Q/R$  (PASSCHIER, in press). Such changes are therefore difficult to detect in the final fabric. For accurate flow analysis, proof should be found that accumulation of volume change happened at a constant rate, or an attempt must be made to estimate variations in  $a$  from relics of early fabric elements. Possibly, data on mean stretching rate (e.g. from palaeopiezometers) or volume change rate (e.g. from crack-seal veins) for the last part of the deformation path can be compared with »mean« values to obtain an estimate of their variability in the same way as described for  $W_n$  above.

### Conclusions

Analysis of the deformation path in naturally deformed rocks can theoretically be carried out on any volume of material which gives evidence of relatively homogeneous deformation on some scale of observa-

tion. For a complete description of the deformation and a reconstruction of the deformation path it is necessary to incorporate data on the flow vorticity number; some methods to determine this number are suggested in this paper. In practice, a lot more research on the effects of flow vorticity number and volume change on microfabric development in rocks is needed before the method can be generally applied; this paper mainly serves to illustrate that fabric elements in naturally deformed rocks, and notably in shear zones, contain more information on the deformation path than is presently being used in structural geology. However, with the criteria given in this paper, some shear zone samples which contain a large number of fabric elements of different age can now be used in analysis of the deformation path (PASSCHIER & URAI, in prep.). Such work can be carried out along the following lines:

- (1) find the orientation of the vorticity vector from the orientation of shape fabric elements and asymmetric microstructures. Only if the vorticity vector coincides with one of the symmetry axes of the finite strain ellipsoid can an accurate analysis be carried out
- (2) construct the Mohr circle for the final position gradient tensor  $F_p$  using:
  - (a) values of stretch and rotation with respect to ISA of three material lines (PASSCHIER & URAI, prep.) or
  - (b) values of finite strain, volume change and »mean«  $W_n$
- (3) determine the variability of  $W_n$  and, if possible, of  $s$  and  $a$
- (4) sketch the domains where the deformation path most probably traversed Mohr space towards the finite position
- (5) carry out controls by application of more than one method for each of the steps given above and by control on the flow pattern in an adjacent, connected domain, e.g. the wall rock in case of a shear zone. An analysis as outlined above can be placed in a wider context if the orientation of the kinematic frame of the flow, e.g. the ISA is known with respect to some external marker.

### Acknowledgements

Thanks to those colleagues who convinced me that Mohr circles are not as stuffy as they seem to be, and to an unknown reviewer for valuable suggestions.

## References

- BELL, T. H. (1985): Deformation partitioning and porphyroblast rotation in metamorphic rocks: a radical reinterpretation. — *J. Metamorphic Geol.*, **3**, 109–118.
- BOBYARCHICK, A. R. (1986): The eigenvalues of steady flow in Mohr space. — *Tectonophysics*, **122**, 35–51.
- CAZES, M., TORREILLES, G., BOIS, C., DAMOTTE, B., GALDEANO, A., HIRN, A., MASCLE, A., MATTE, P., VAN NGOC, P. & RAOULT, J.-F. (1985): Structure de la croûte hercynienne du Nord de la France: premiers résultats du profil ECORS. — *Bull. Soc. géol. France*, **8**, 925–941.
- DE PAOR, D. G. (1983): Orthographic analysis of geological structures — I. Deformation theory. — *J. Struct. Geol.*, **5**, 255–278.
- & MEANS, W. D. (1984): Mohr circles of the first and second kind and their use to represent tensor operations. — *J. Struct. Geol.*, **6**, 693–701.
- DIETRICH, D. & SONG, H. (1984): Calcite fabrics in a natural shear environment, the Helvetic nappes of Switzerland. — *J. Struct. Geol.*, **6**, 19–32.
- DURNEY, D. W. & RAMSAY, J. G. (1973): Incremental strains measured by syntectonic crystal growths. — In: *Gravity and Tectonics*, 67–96.
- ELLIOTT, D. (1972): Deformation paths in structural geology. — *Geol. Soc. Am. Bull.*, **83**, 2621–2638.
- FREEMAN, B. (1985): The motion of rigid ellipsoidal particles in slow flows. — *Tectonophysics*, **113**, 163–183.
- GHOSH, S. K. (1987): Measure of non-coaxiality. — *J. Struct. Geol.*, **9**, 111–115.
- & RAMBERG, H. (1976): Reorientation of inclusions by combination of pure and simple shear. — *Tectonophysics*, **34**, 1–70.
- HUTTON, D. H. W. (1982): A tectonic model for the emplacement of the main Donegal granite, NW Ireland. — *J. geol. Soc. London*, **139**, 615–631.
- KREIDER, D. L., KULLER, R. G. & OSTBERG, D. R. (1972): *Elementary differential equations*, Addison-Wesley Publishing Company.
- LAW, R. D., KNIPE, R. J. & DAYAN, H. (1984): Partitioning within thrust sheets; microstructural and petrofabric evidence from the Moine thrustzone at Loch Eriboll, NW Scotland. — *J. Struct. Geol.*, **6**, 477–498.
- LISTER, G. S. & HOBBS, B. E. (1980): The simulation of fabric development during plastic deformation and its application to quartzite: the influence of deformation history. — *J. Struct. Geol.*, **2**, 355–371.
- & WILLIAMS, P. F. (1983): The partitioning of deformation in flowing rock masses. — *Tectonophysics*, **92**, 1–33.
- & SNOKE, A. W. (1984): S-C Mylonites. — *J. Struct. Geol.*, **6**, 617–638.
- MCKENZIE, D. P. (1979): Finite deformation during fluid flow, *Geophys.* — *J. R. Astron. Soc.*, **58**, 689–715.
- MALVERN, L. E. (1969): *Introduction to the mechanics of a continuous medium*, Prentice Hall, Englewood Cliffs. — N.J.
- MEANS, W. D. (1981): The concept of steady state foliations. — *Tectonophysics*, **78**, 179–199.
- (1982): An unfamiliar Mohr circle construction for finite strain. — *Tectonophysics*, **80**, T1–T6.
- (1983): Application of the Mohr-circle construction to problems of inhomogeneous deformation. — *J. Struct. Geol.*, **5**, 279–286.
- , HOBBS, B. E., LISTER, G. S. & WILLIAMS, P. F. (1980): Vorticity and non-coaxiality in progressive deformations. — *J. Struct. Geol.*, **2**, 317–378.
- PASSCHIER, C. W. (1986a): Mylonites in the continental crust and their role as seismic reflectors, *Geologie en Mijnbouw*, **65**, 167–176.
- (1986b): Flow in natural shear zone — the consequences of spinning flow regimes. — *Earth Plan. Sci. Letters*, **77**, 70–80.
- (1987a): Efficient use of the velocity gradients tensor in flow modelling. — *Tectonophysics*, **136**, 159–163.
- (1987b): Stable positions of rigid objects in non-coaxial flow — a study in vorticity analysis, *J. Struct. Geol.*, **9**, 419–427.
- (1988): The use of Mohr circles to describe non-coaxial flow regimes and resulting deformation in rocks, submitted to *Tectonophysics*.
- & SIMPSON, C. (1986): Porphyroclast systems as kinematic indicators. — *J. Struct. Geol.*, **8**, 831–843.
- & URAI, J. (1988): Vorticity and strain analysis using floating Mohr diagrams. — Submitted to *Geology*.
- PLATT, J. P. & BEHRMANN, J. H. (1986): Structures and fabrics in a crustal scale shear zone, Betic Cordillera, SE Spain. — *J. Struct. Geol.*, **8**, 15–35.
- RAMBERG, H. (1975a): Superposition of homogeneous strain and progressive deformation in rocks. — *Bull. Geol. Inst. Univ. Uppsala, N.S.*, **6**, 36–67.
- (1975b): Particle paths, displacement and progressive strain applicable to rocks, *Tectonophysics*, **28**, 1–37.
- SCHONEVELD, C. (1977): A study of some typical inclusion patterns in strongly paracrystalline-rotated garnets. — *Tectonophysics*, **39**, 453–471.
- SIMPSON, C. & SCHMID, S. M. (1983): An evaluation of criteria to deduce the sense of movement in sheared rocks. — *Bull. geol. Soc. America*, **94**, 1281–1288.
- SMITHSON, S. B., BREWER, J. A., KAUFMAN, S., OLIVER, J. E. & HURICH, C. A. (1979): Structure of the Laramide Wind River uplift, Wyoming, from COCORP deep reflection data and from gravity data. — *J. Geoph. Res.*, **B-84**, 5955–5972.
- SMYTHE, D. K., DOBINSON, A., MCQUILLIN, R., BREWER, J. A., MATTHEWS, D. H., BLUNDELL, D. J. & KELK, B. (1982): Deep structure of the Scottish Caledonides revealed by the Moist reflection profile. — *Nature*, **299**, 338–340.
- TRUESDELL, C. (1954): *The kinematics of vorticity*. — Indiana University Press, Bloomington, Ind.
- TALBOT, C. J. (1970): The minimum strain ellipsoid using deformed quartz veins. — *Tectonophysics*, **9**, 46–76.